 FDMP, vol.8, no.2, pp.155-172, 2012

Numerical and Analytical Analysis of the Thermosolutal Convection in an Heterogeneous Porous Cavity

K. Choukairy[1] **and R. Bennacer**[2]

Abstract: This study carries the natural thermosolutal convection induced in heterogeneous porous media. The configuration considered is cartesian. The horizontal and vertical walls are submitted to different mass and heat transfer. The equations which govern this type of flow are solved numerically by using the finite volume method. The flow is considered two-dimensional and laminar. The model of Darcy and the approximation of the Boussinesq are taken into account. The parameters which control the problem are the thermal Darcy-Rayleigh number, Rt, the buoyancy ratio, N, the Lewis number, Le, the aspect ratio of the enclosure, A and the local permeability ratio, K_r. The flow fields, temperature and concentration are given for various values of the local permeability. The effects of increasing the local permeability, the thermal Darcy-Rayleigh number Rt and buoyancy ratio, N on the heat and mass transfer are discussed. These numerical results were confirmed analytically by using the parallel flow approximation. A good agreement was found between the two analytical and numerical approaches, which confirm the validity of the analytical approach in such heterogeneous domain. The flow intensity and transfer increase with the increase of the permeable heterogeneity of the domain.

Keywords: Natural convection, heterogeneous, porous media, thermosolutal, parallel flow, bifurcation.

Nomenclature

A	aspect ratio of the enclosure, L/H
a	lateral heating intensity
b	constant controlling the permeability heterogeneity, Eq. (5)
C_S	dimensionless concentration gradient in x-direction

[1] Université Hassan 1 SETTAT, Laboratoire MMII, Equipe Energétique. Ecole Nationale des sciences appliquées Khouribga

[2] Ecole Normale Supérieure (ENS)-Cachan - Dpt. GC/ LMT/CNRS UMR 8535

C_T dimensionless temperature gradient in x-direction
g gravitational acceleration
H height of the enclosure
j constant mass flux per unit area
K_r dimensionless resistivity of the porous medium
K_0^r reference resistivity
L width of the cavity
Le Lewis number, α/D
N buoyancy ratio, $\beta_s \Delta S/\beta_T' \Delta T'$
Nu Nusselt number
q constant heat flux, per unit area
Rt thermal Rayleigh number
S dimensionless concentration $(S' - S_\alpha{}') / \Delta S'$
Sh Sherwood number
T dimensionless temperature, $(T' - T_0') / \Delta T'$
(u, v) dimensionless velocity, $(u'/(\alpha/H), v'/(\alpha/H))$
(x, y) dimensionless coordinate system, $(x'/H, y'/H)$

Greek symbol

α fluid thermal diffusivity, $\lambda/(\rho C)_f$
β_s solutal expansion coefficient
β_T thermal expansion coefficient
ν kinematic viscosity
ρ fluid density
$(\rho C)_f$ fluid heat capacity
$(\rho C)_p$ saturated porous medium heat capacity
σ heat capacity ratio, $(\rho C)_p/(\rho C)_f$
Ψ dimensionless stream function, Ψ'/α
Ψ_0 dimensionless stream function at the center of the cavity

Subscript

S solutal
0 refers to the center of the cavity
T temperature

1 Introduction

Natural convection in fluid saturated porous media occurs in many engineering systems and in nature. It includes the disposal of waste material, drying processes, migration of moisture contained in fibrous insulation, grain storage installations, food processing, chemical transport in packed-bed reactors, contamination transport in saturated soil, etc., see for instance Alavyoon (1991), Aouachria (2009), M.Er-Raki(2009) and Montel (1994). Most investigation of this topic are concerned with the case of isotropic porous media with different configuration (Cartesian, Cylindrical) in transient and steady state, Prasad (1986), Hasnaoui (1995), K.Choukairy (2006), Bennacer (2003), Achoubir (2008) and Choukairy (2006). However, in several applications the porous materials present macroscopically heterogeneity or anisotropy. Natural convection in such heterogeneous porous media has received relatively little attention despite its broad range of applications. Castinel and Cambarnous (1994) have considered the variable permeability for the study the flow through a porous medium. Both experimental and theoretical results were reported by those authors for the case of a layer with impermeable boundaries. The same configuration was considered by McKibbin (1984), Nilsen and Storesletten (1990), Bennacer (2001), Bennacer and El Ganaoui (2004) for various boundary conditions.

The study of such effect on the mixed convection in semi infinite porous medium bounded by horizontal surfaces has been considered by Hassanien (2003). It was found that a variable permeability tends to increase the heat transfer rate. The effect on an anisotropic permeability of arbitrary orientation on the convective heat transfer in a vertical cavity heated isothermally from the sides was investigated numerically by Zhang (1993). The same configuration was considered by Degan (1998) for the case of constant applied heat fluxes on the vertical walls of the enclosure. The results indicate that a maximum (minimum) heat transfer occurs when the porous matrix is oriented with its principal axis with higher permeability parallel (perpendicular) to the vertical direction.

The main purpose of this work is to study the natural convection in a porous layer incorporating the permeability variation especially the increase close to the horizontal surfaces. The horizontal and vertical walls are maintained at different mass and heat conditions. The parallel flow approximation was applied and validated numerically using finite-volume approach.

2 Mathematical model

Consider a fluid-saturated, porous layer enclosed in a rectangular cavity of length L and height H as illustrated on Fig.1. The origin of the coordinate system is located

at the center of the cavity. The two horizontal walls of the cavity are exposed to uniform heat (q) and solute (j) fluxes. The vertical walls are subjected to uniform heat flux (a x q), where a is constant values. All the boundaries are impermeable. It is assumed that the flow is incompressible laminar and the fluid is Newtonian.

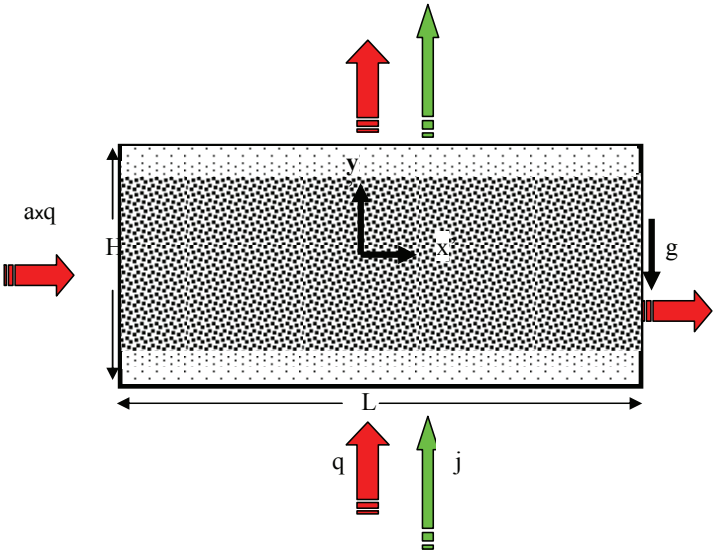

Figure 1: Geometry of the problem

The problem is considered as two-dimensional. The Boussinesq approximation is assumed to be valid. The thermo physical properties of the fluid are assumed to be constant, except the density ρ of the mixture is related to the temperature and solute concentration by a linear equation of state:

$$\rho\left(T',S'\right)=\rho_r\left[1-\beta_T(T'-T'_0)-\beta_S(S'-S'_0)\right] \tag{1}$$

where β_T and β_S are the thermal and solutal relative density variation respectively and ρ_r is the reference density computed at $T'=T_0'$ and $S'=S_0'$.

The porous matrix is assumed to be rigid and in thermal equilibrium with the fluid.

The dimensionless equations describing conservation of momentum, energy and concentration are given respectively by:

$$\frac{\partial u}{\partial x}+\frac{\partial v}{\partial y}=0 \tag{2}$$

$$\nabla\left[1/K_r(y)\nabla\psi\right]=-Rt\frac{\partial(T+NS)}{\partial x} \tag{3}$$

$$u\frac{\partial T}{\partial x}+v\frac{\partial T}{\partial y}=\nabla^2 T \tag{4}$$

$$u\frac{\partial S}{\partial x}+v\frac{\partial S}{\partial y}=Le^{-1}(\nabla^2 S) \tag{5}$$

In the present study it is assumed that the permeability of the porous medium changes with the depth, increasing from the bulk to the horizontal surfaces of the layer in the following way Fig.2:

$$K_r(y)=1+4*(2*y)^n=1+4*(2*y)^{1/b} \tag{6}$$

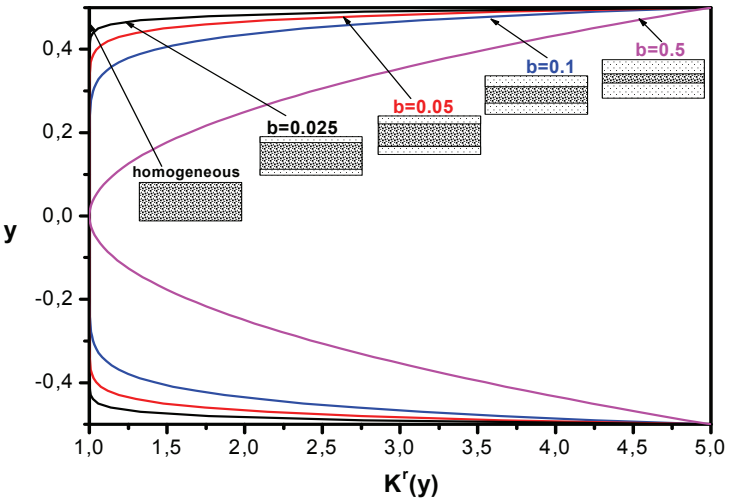

Figure 2: Permeability of the porous media versus the depth for different b values.

The above equations were obtained using the following dimensionless quantities

$$(x,y)=\frac{(x',y')}{H}\quad (u,v)=\frac{(u',v')H}{\alpha} \tag{7}$$

$$T=\frac{(T'-T_0{}')}{\Delta T}\ \text{where}\ \Delta T'=\frac{qH}{\lambda} \tag{8}$$

$$S=\frac{(S'-S_0{}')}{\Delta S}\ \text{where}\ \Delta S'=\frac{jH}{D} \tag{9}$$

$$\psi=\frac{\psi'}{\alpha}\quad K_r(y)=\frac{K'(y)}{K_r^0}\quad \varepsilon=\frac{\Phi}{\sigma} \tag{10}$$

where α is the fluid mixture thermal diffusivity, σ heat capacity ratio, λ the thermal conductivity, q and j are respectively the constant heat and mass fluxes applied on the system. K' is permeability of the porous medium, K_r^0 the reference resistivity at the center of the layer and ϕ the porosity of the porous medium.

The stream function ψ' is defined by: $u' = -\frac{\partial \psi'}{\partial y'}$ and $v' = \frac{\partial \psi'}{\partial x'}$, such that the conservation of mass is satisfied.

The dimensionless parameters that characterize the problem in the equations (4)-(6) are:

$$Rt = \frac{g\beta \Delta T H}{K\alpha\nu}, \quad N = \frac{Gr_s}{Gr_T} = \frac{\beta_S}{\beta_T}\frac{\Delta S'}{\Delta T'}, \quad A = \frac{L}{H} \tag{11a}$$

$$Le = \frac{Sc}{Pr} \tag{11b}$$

where $Pr = \frac{\nu}{\alpha}$ and $Sc = \frac{\nu}{D}$,

where Rt, N, A and Le are the thermal Darcy-Rayleigh number, the solutal to thermal buoyancy ratio, the domain aspect ratio and the Lewis number, respectively.

The dimensionless boundary conditions on the vertical walls and horizontal surfaces are as follows:

$$x = \pm\frac{A}{2} \quad \frac{\partial T}{\partial x} = a\psi = 0 \quad \frac{\partial S}{\partial x} = 0 \tag{12a}$$

$$y = \pm\frac{1}{2} \quad \frac{\partial T}{\partial y} = -1 \quad \psi = 0 \quad \frac{\partial S}{\partial y} = -1 \tag{12b}$$

The Nusselt and Sherwood numbers are evaluated by:

$$Nu = \frac{1}{\triangle T} \tag{13a}$$

$$Sh = \frac{1}{\triangle S} \tag{13b}$$

where $\triangle T = \left(T\left(x, -\frac{1}{2}\right) - T\left(x, +\frac{1}{2}\right)\right)$ and $\triangle S = \left(S\left(x, -\frac{1}{2}\right) - S\left(x, +\frac{1}{2}\right)\right)$ are, the average temperature and concentration difference between the two horizontal surfaces, respectively.

3 Numerical method

The governing equations (2) to (5) were solved by using the control volume finite difference method described by Patankar (1980). SIMPLER algorithm is employed to solve the equations in primitive variables.

Non uniform grids are used in the program, allowing fine grid spacing near the boundaries. Calculations were necessary to check the accuracy. Convergence with mesh size was verified by employing coarser and finer grids on selected test problems. The typical grid points in the present study were (101 x 51).

The convergence criterion was based on the average residue of the continuity equation and the average quadratic residues of each governing equation evaluated on the whole computational domain. It was assumed that convergence was reached when the maximum error was within machine error (10^{-9}).

The computer code was validated with the result available in literature Marcoux (1990) (Tab.1). The comparison was observed to be very good with a maximum deviation of less than 1%.

Table 1: Comparison of our results with MARCOUX (1999). Le = 10, N = 1

Present work	*Nu* Sh	4,02 14,39	Rt=50
Marcoux *(1999)*	*Nu* Sh	3,98 14,37	
Present work	*Nu* Sh	5,43 18,14	Rt=100
Marcoux *(1999)*	*Nu* Sh	5,42 18,11	

The Tab.2 determine the minimum aspect ratio above which the flow can be assumed to be parallel, it was found that the numerical results can be considered independent of aspect ratio for $A \geq 6$. Most of the numerical results presented in this study were obtained for A=6.

Table 2: The effects of the aspect ratio A, on the obtained parallel flow for different values of b

b		A=2	A=3	A=6	A=8	Analytical
0	Ψ_{cen} Nu	-0.61 1.17	-0.79 1.27	-0.81 1.31	-0.81 1.31	-0.81 1.31
0.05	Ψ_{cen} Nu	-1.12 1.60	-1.25 1.82	-1.26 1.88	-1.26 1.88	-1.26 1.90
0.1	Ψ_{cen} Nu	-1.36 1.92	-1.50 2.23	-1.51 2.31	-1.51 2.31	-1.514 2.33

Fig.3 illustrates the iso-levels of the stream function, isotherm and isoconcentration obtained numerically for Rt=15, N=0.1, a=0.05, Le=10 and different values of b. Fig. 3(a) represent the homogeneous cases (b=0), and Fig.3(b,c) characterize the heterogeneous cases. From these results, it's observed that the flow is parallel for the different obtained cases. The temperature and concentration gradient in the horizontal direction is observed to remain constant in the central region of the cavity.

For the first case (Fig.3(a)), we observe a symmetrical horizontal flow, the temperature and concentration field is centro-symmetric. For the heterogeneous cases, due to the increase of domain permeability in the same way near the top and bottom surfaces (Fig.2), we observe also symmetrical horizontal parallel flow but the value of ψ and Nu increases from $(\psi = 0.824, Nu = 1.26)$ for b=0 to $(\psi = 1.614, Nu = 2.345)$ for b=0.1, indicating that the strength of the convective circulation within the cavity is promoted when we increases the values of b.

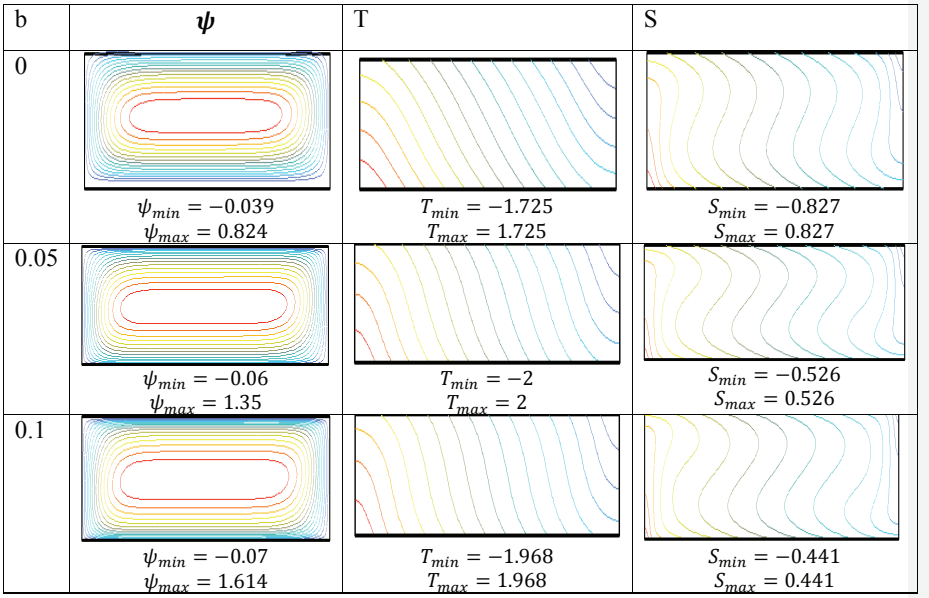

Figure 3: Iso-lines of stream-function temperature and concentration for different b value

4 Analytical Solution

In this section, an analytical solution is developed for the case of A>>1, by using the parallel flow approximation.

For this situation, we have:

$$\Psi(x,y) \approx \Psi(y) \tag{14}$$

$$T(x,y) = C_T x + \theta_T(y) \tag{15}$$

$$S(x,y) = C_S x + \theta_S(y) \tag{16}$$

where C_T and C_S are unknown constant temperature and concentration gradients, in x-direction, and θ_T and θ_S are the temperature and concentration profiles in the vertical direction, respectively.

Substituting Eqs. (14-16) into Eqs. (3-5) yields the following set of equations:

$$\frac{1}{K_r(y)}\frac{d^2\Psi}{dy^2}+\frac{d}{dy}\left(\frac{1}{K_r(y)}\right)\frac{d\Psi}{dy}=-E \tag{17}$$

$$\frac{d^2\theta_T}{dy^2}=C_T\frac{d\Psi}{dy} \tag{18}$$

$$\frac{d^2\theta_S}{dy^2}=LeC_S\frac{d\Psi}{dy} \tag{19}$$

where

$$E=Rt(C_T+NC_S) \tag{20}$$

According to Kimura (1995), the equivalent energy flux condition in x-direction for the temperature and concentration are given by:

$$C_T+a=\int_{-1/2}^{+1/2}u\theta_T dy \tag{21}$$

$$C_S=\int_{-1/2}^{+1/2}u\theta_S dy$$

The analytical solutions of Equations (17-19), subject to the boundary conditions (12), give the following results:

$$\left.\begin{array}{l}\psi(y)=A_1y^{1/b+2}+B_1y^2+C_1\\ T(y)=A_2y^{1/b+3}+B_2y^3+C_2y\\ S(y)=A_3y^{1/b+3}+B_3y^3+C_3y\end{array}\right\} \tag{22}$$

where A_i, B_i and C_i are constants, their values are given in appendix.

The solution of the equation (21), enables us to find constant C_T and C_S:

$$\left.\begin{array}{r}C_T=\frac{-D_1a-G_1}{D_1+F_1E^2}\\ C_s=H_1\frac{LeE}{D_1+F_1E^2Le^2}\end{array}\right\} \tag{23}$$

where D_1, F_1, G_1 and H_1 are constants; their values are given in appendix for each value of b.

Upon combining equations (23) and (20), it's found that:

$$\alpha_0 + \alpha_1 E + \alpha_2 E^2 + \alpha_3 E^3 + \alpha_4 E^4 + \alpha_5 E^5 = 0 \tag{24}$$

$$\int_{i=0}^{5} \alpha_i E^i = 0$$

Where:

$$\left.\begin{array}{c} \alpha_5 = K * Le^2 \\ \alpha_4 = 0 \\ \alpha_3 = 2 * Rt * \left(-C * N * le - C * Le^2\right) + 2 * D * (1 + Le^2) \\ \alpha_2 = 2 * D * Rt * a * Le^2 \\ \alpha_1 = -F * Rt * (1 + N * Le) + G \\ \alpha_0 = G * Rt * a \end{array}\right\} \tag{25}$$

where *K,C,D,F,G* are constants; (see appendix for each value of b).

Having the value of Rt, Le, N and *a*, the equation (24) is resolute by using the Muller's method in order to get the different values of $\boldsymbol{E}$.

The corresponding Nusselt and Sherwood numbers along the vertical walls are:

$$\left.\begin{array}{l} Nu = \frac{-1}{-1+\xi E C_T} \\ Sh = \frac{-1}{-1+\xi E Le C_S} \end{array}\right\} \tag{26}$$

where ζ is constant value (given in appendix).

For y=0, the equation (22a) became $\psi(y) = \psi_0 = C_1 = \rho.E$ (where ρ is constant, see appendix for each value of b)

By replacing ψ_0 in the equation (24) and for the case of a=0 (i.e. without lateral heating), the equation (24) becomes:

$$\psi_0 (Le^4 {\psi_0}^4 - 2le^2 \phi_1 {\psi_0}^3 - \phi_2) = 0 \tag{27}$$

Where $\phi_1 = \frac{-\alpha_1 Le^2}{K}$ and $\phi_2 = \frac{-\alpha_3}{2K}$.

The solution for the equation (26) is expressed as follows:

$$\psi_0 = \left\{ \pm \frac{1}{Le} (\phi_1 \pm \sqrt{\phi_1^2 + \phi_2})^{\frac{1}{2}}, 0 \right\} \tag{28}$$

The equation (28) represents the pure conduction solution rest state $\psi_0 = 0$, and four other solutions stand for convective solutions. The equation (28) allows us to find the critical values of existence of convective flow in the layer. The supercritical

Rayleigh number Rt_c^{sup}, for the onset of motion is obtained, when the condition $\phi_1 < 0$ and $\phi_2 = 0$ are satisfied, as

$$Rt_c^{sup} = \frac{G}{F(1+NLe^2)} \tag{29}$$

The distribution of velocity component (u), temperature (T) and concentration (S) profiles in the vertical mid-plane of the cavity for different values of heterogeneous resistivity parameter b and for Rt=15, N=0.1, Le=10, a=0.05 are represented on Fig.4. The numerical results are represented by dotted symbols on the other hand the analytical results by solid lines. The results show that two results (analytical and numerical) are in excellent agreement. These profiles are anti-symmetrical for all values of b (Eqt.5). The homogeneous cases (b=0) correspond to a porous layer with a constant permeability for which the velocity, temperature and concentration profiles varies linearly with y with respect to the center of the layer. Such linear velocity behavior is a consequence slip boundary condition and Darcy flow. As the values of b is increased, the flow resistance is lower in the top and bottom part of the layer the flow intensity is promoted in this region Fig.4a. As a result, Fig.4b-c indicates that both the temperature and concentration increase at the top and the bottom of the layer.

Fig. 5 illustrates the effect of the Rayleigh number Rt and b on Nu and Sh for a=0.05, Le=10 and for two values of the buoyancy ratio N (N=0.1, N=-0.1).

For Fig.5a, and for Rt$<$0, the heat and mass effect are cooperating, and they are in the same direction as the forces of gravity, so the fluid is at rest state with corresponding diffusive heat and mass transfer like shows it the isotherm and isoconcentration in top graphs. When Rt$>$0, the heat and mass effect are cooperating, and they are in the opposite direction as the forces of gravity, the flow is destabilizing.

For Fig.5b, the mass and heat effect are acting in opposite direction. For Rt$<$0, the heat transfer and the forces of gravity are in the same direction, so the heat transfer is stabilizing, what corresponds to a diffusive transfer (see the isotherm in top graphs), on the other hand the mass transfer is destabilizing. When Rt$>$0, the heat transfer and the forces of gravity are in the opposite direction, so the heat transfer is destabilizing, on the other hand the mass transfer and the forces of gravity are in the same direction, so the mass transfer is stabilizing.

The influence of parameter b on the heat and mass transfer rates is observed to be significant. Thus, it's observed that the increase of b from 0 to 0.1, the heat and mass transfer are doubled and it's more interesting for N=0.1. All the curves indicate that the mass transfer tend asymptotically toward constant values that depend upon the variable permeability parameter b.

Fig.6(a-b) exemplify the bifurcation diagram in terms of Ψ_{ext} for various values

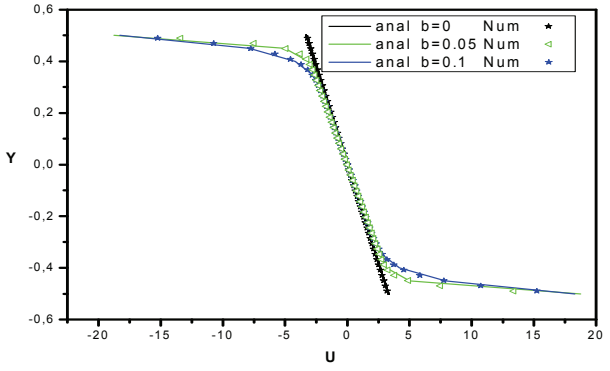

(a)

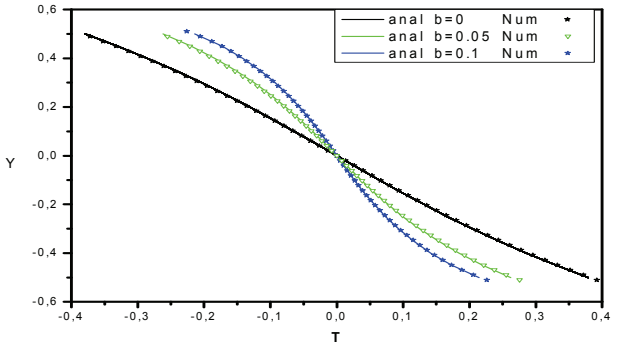

(b)

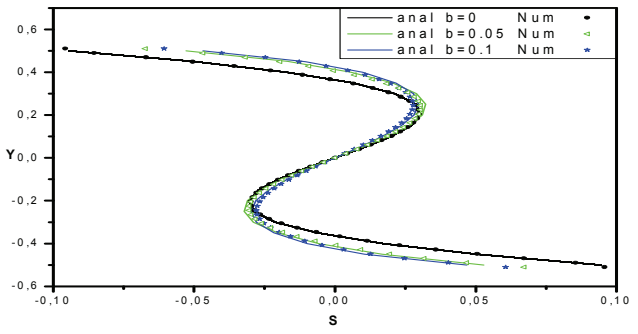

(c)

Figure 4: Profiles of Horizontal velocity component (a), Temperature(b) and Concentration(c) in the vertical mid-plan for different values of b (Rt = 15).

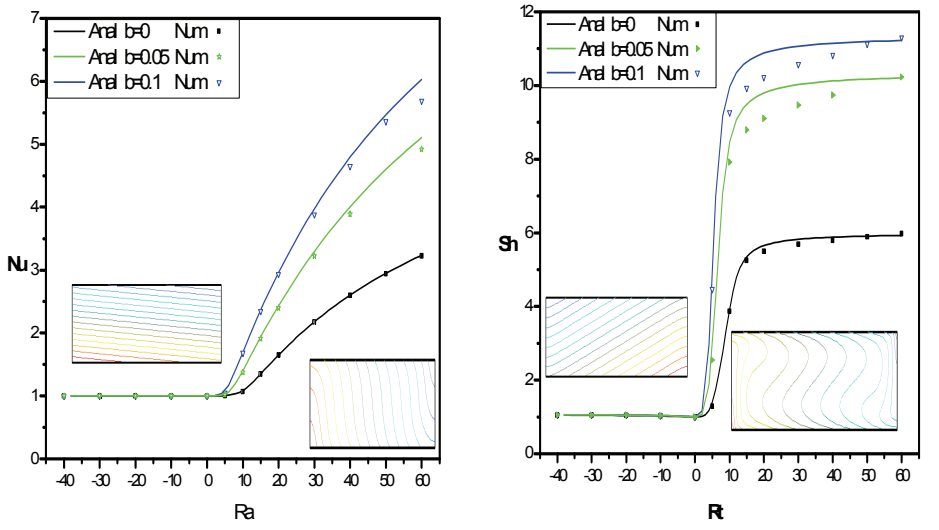

(a)

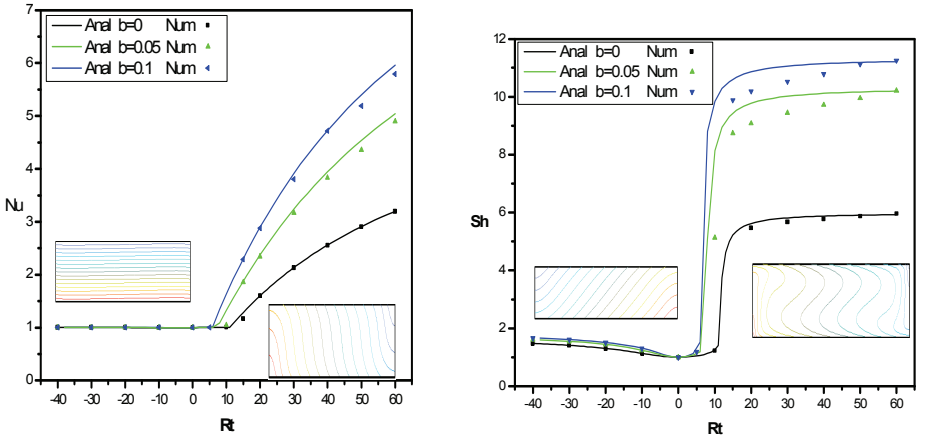

(b)

Figure 5: Effect of Rt and b on the Nusselt Number Nu and Sherwood number Sh for N=0.1 (a) and N=-0.1(b)

of b for N=0.1 and N=-0.1. The curves depicted in these graphs are the predictions of the parallel flow approximation. The numerical solution of the full governing equation, depicted by dots is in good agreement with the analytical solution. Fig6.a, presents the case of the solute is destabilizing, for this situation, the onset of motion occurs through a pitchfork bifurcation. For the case of a homogeneous porous media (b=0), the onset of motion occurs at $Rt_c^{sup} = 6$. As the heterogeneity of the porous layer, the onset of motion occurs at $Rt_c^{sup} = 3,94$ for b=0.05 and $Rt_c^{sup} = 3,12$ for b=0.1. So, the onset of motion occurs as the values of permeability increases. Typical results, obtained for the case N=-0.1, in which the solute is stabilizing, are representing in Fig6.b.

Fig.7 represents the variation of Rt_c^{sup} according to the buoyancy ratio N for different values of b, we can notice that the critical Rayleigh number decreases considerably as the value of b increases. This follows that from the fact that an increase of b corresponds to increases the permeability in the top and bottom of porous layer. The Fig.7 shows that the onset of motion from the rest state depend on N. As the value of N increase the critical Rayleigh number tends to asymptotically toward zero. For classical case on a homogeneous porous layer, and for N=0, the curve is observed to tend asymptotically toward the limit $Rt_{sup} = 12$, as predicted in the past by Nield (1999).

5 Conclusion

In this paper, the effect of the hydraulic heterogeneity on natural convection in a rectangular cavity is investigated. The two horizontal walls of the cavity are exposed to uniform heat and solute fluxes. The vertical walls are subjected to uniform heat flux. Based on the parallel flow approach, an analytical solution for the stream function, the temperature and the concentration are established for different values of b. This result shows a good agreement with a numerical result. The influence of the Rayleigh number, inhomogeneity b and the buoyancy ratio N on the Strength of convection (ψ_{ext}), Nusselt number (Nu) and Sherwood number (Sh) are also analyzed numerically and analytically. The existence of multiples solutions, for given values of the governing parameters, are demonstrated. It's found that the heat and mass transfer are doubled while passing from the homogeneous case (b=0) to the heterogeneous case (b=0.05, b=0.1). The critical Rayleigh number for the onset of motion in a horizontal layer is also predicted by the present analytical study for different values of b.

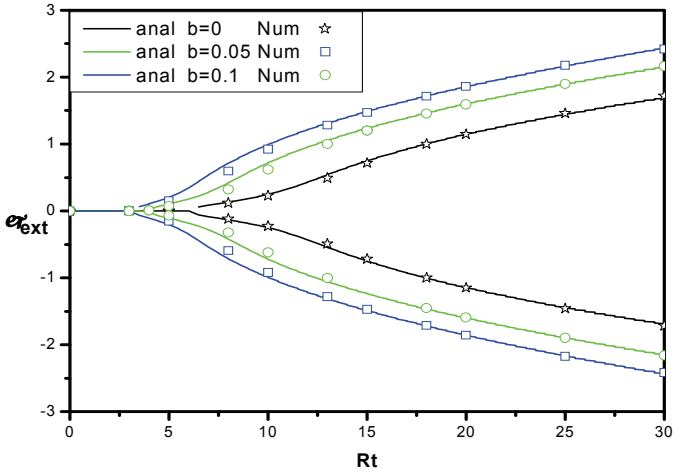

(a)

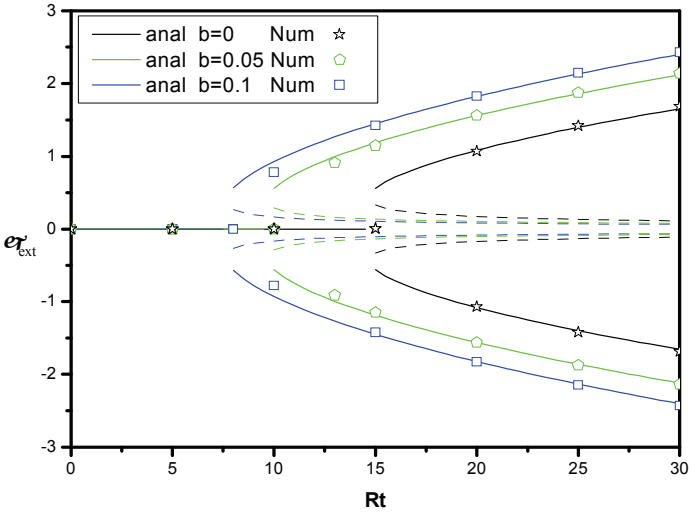

(b)

Figure 6: Bifurcations diagrams in terms of ψ_{ext} for a=0, Le=10 and two values of N (N=0.1 (a) and N=-0.1 (b))

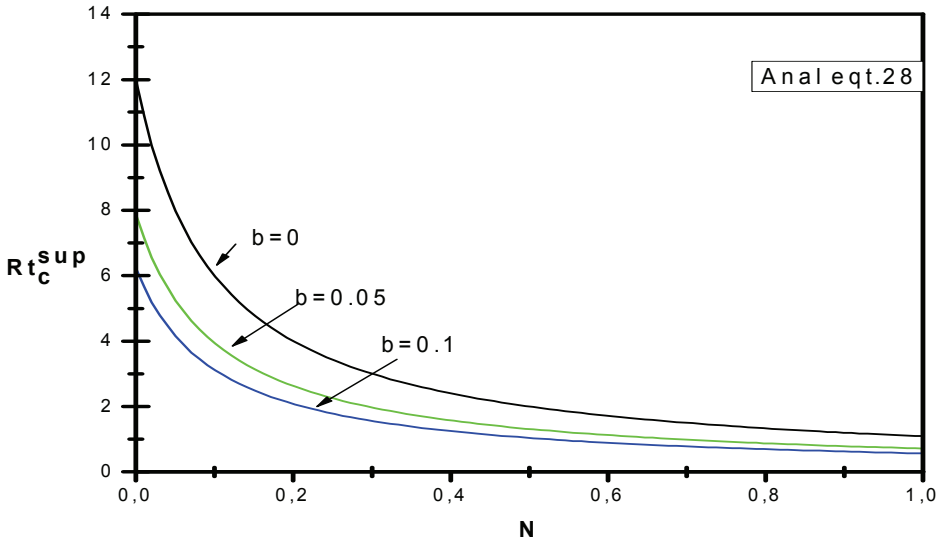

Figure 7: Effects of N and b on the supercritical Rayleigh number, for the onset of motion

References

Alavyoon,F.; Eklund,A.; Bark,F.H.; Simonsson,D; (1991): Theoretical and experimental studies of free convection and stratification of electrolyte in a lead-acid cell during recharge. *I. Electrochim. Acta*; vol. 14, pp. 2153-2164.

Aouachria Z, (2009): Heat and Mass Transfer Along of a Vertical Wall by Natural convection in Porous Media, *Fluid Dyn. Mater. Process*., vol. 5, no. 2, pp. 137-148.

Achoubir K.; Bennacer R.; Cheddadi A.; El Ganaoui M.; and Semma E., (2008), Numerical Study of Thermosolutal Convection in Enclosures Used for Directional Solidification (Bridgman Cavity), *Fluid Dyn. Mater. Process*., vol. 4, no. 3, pp. 199-210.

Bennacer,R.; Beji,H.; Mohamad, A.A; (2003): Double Diffusive Natural Convection in a Vertical Multilayer Saturated Porous Media, *International Journal of Thermal Sciences*.: vol. 42, pp. 141-151.

Bennacer, R.; Tobbal, A.; Beji,H. ; Vasseur ,P. (2001): Double Diffusive Convection In A Vertical Enclosure Filled With Anisotropic Porous Media , *Int. J. of Thermal Sciences*; vol. 40, no. 1, pp. 30-41.

Bennacer, R.; El Ganaoui, M. and Fauchais, P. (2004): On the thermal anisotropy affecting transfers in a multilayer porous medium. *Comptes Rendus Mecanique*, vol. 332, no. 7, July 2004, pp. 539-546.

Castinel, G.; Combarnous, M. (1974): Critére d'apparition de la convection naturelle dans une couche poreuse anisotrope, *C. R. Acad. Sci. Paris*, vol. B278, pp. 701-704.

Choukairy,K; Bennacer,R.; (2006): The effects of porous block on transient natural convection, *Mecanique and Industrie*, vol. 7, pp. 573-578.

Degan ,G.;Beji ,H.;Vasseur, P. ; Robillard,L. ; (1998) Effects of anisotropy on the development of convective boundary layer flow in porous media, *Int. Comm. Heat Mass Transfer*, vol. 25, no. 8, pp. 1159-1168.

Hasnaoui, H.;Vasseur, P.; Bilgen,E.; Robillard, L. (1995): Analytical and numerical study of natural convection heat transfer in a vertical porous annulus. *Chem. Eng. Comm.*, vol. 131, pp. 141-159.

Hassanien, I.A; Salama, A.A.; Elaiw, A.M. (2003): Variable permeability effect on vortex instability of mixed convection flow in a semi-infinite porous medium bounded by a horizontal surface. *App. Math. Comp.*, vol. 146, pp. 829-847.

Choukairy, K.; Bennacer, R.; Beji, H.; El Ganaoui, M.; Jaballah, S. (2006): Transient Behaviours Inside A Vertical Cylindrical Enclosure Heated from The Side Walls. *Num. Heat Transfer part A*, vol. 50, pp. 1-13.

Kimura, S.; Vynnycky, M.; Alavyoon, F. (1995): Unicellular natural circulation in a shallow porous layer heated from below by a constant flux, . *J. Fluid Mech.*, vol. 24, pp. 231-2

Marcoux M.; Charrier-Mojtabi, M.; Azaiez, M.; (1999): Double diffusive convection in an annular vertical porous layer. *Int. J. Heat Mass Transfer*, vol. 42, pp. 2313-2325.

McKibbin, R. (1984): Thermal convection in a porous layer: effects of anisotropy and surface boundary conditions, *Trans. Porous Media*, vol. 1, pp. 271-292.

Er-Raki, M. ; Hasnaoui, M.; Amahmid, A.; El Ganaoui, M. (2009): Computational study of a thermosolutal convection problem within a vertical porous enclosure in the particular case of a buoyancy ratio balancing the separation parameter. *International Journal of Thermal Sciences (IJTS),* vol. 48, no. 6, pp. 1129-1137.

Montel, F. (1994): Importance de la thermodiffusion en exploration et production petrolieres. *Entropie*; vol. 184/185, pp. 86-93.

Nield, D.A.; Bejan, A. (1999): A convection in porous media. *2Ed.Springer, Berlin.*

Nilsen, T.; Storesletten, L. (1990): An analytical study on natural convection in

isotropic and anisotropic porous channels, *J. Heat and Transfer*, vol. 112, pp. 396-401.

Patankar, S. (1980): Numerical heat transfer and fluid flow. Hemisphere, Washington, DC.

Prasad, V.; Kulacki, F.A.; Kulkarni, A.V. (1986): Free convection in a vertical porous annulus with constant heat flux on the inner wall: experimental results. *Int. J. Heat Mass Transfer*, vol. 29, pp. 713-723.

Zhang, X. (1993): Convective Heat Transfer In A Vertical Porous Layer With Anisotropic Permeability, Proc. 14^{th} Canadian Congr. *Applied Mechanics,* vol. 2, pp. 579-580.

Appendix

b=	A_1	B_1	C_1	A_2	B_2	C_2
0.1	$\frac{-2048}{6}E$	$-\frac{1}{2}E$	$\frac{5}{24}E$	$\frac{-1024}{39}C_tE$	$-\frac{1}{6}C_tE$	$\frac{5}{24}C_tE+b$
0.05	$\frac{-4194304}{22}E$	$-\frac{11}{22}E$	$\frac{15}{88}E$	$\frac{-2097152}{253}C_tE$	$\frac{-253}{1518}C_tE$	$\frac{15}{88}C_tE+b$
0	0	$-\frac{1}{2}E$	$\frac{1}{8}E$	0	$-\frac{1}{6}C_tE$	$\frac{1}{8}C_tE+b$

b=	A_3	B_3	C_3
0.1	$-\frac{2048}{78}LeC_SE$	$-\frac{13}{78}LeC_SE$	-1+5/24LeCsE
0.05	$-\frac{2097152}{253}LeC_SE$	$-\frac{1}{6}LeC_SE$	-1+15/88LeCsE
0	0	$-\frac{1}{6}LeC_SE$	-1+1/8LeCsE

b=	D_1	F_1	G_1	H_1	ζ
0.1	23400	659	3750E	3750	25/156
0.05	41400	737	5250E	5250	35/276
0	120	1	10E	10	1/12

b=	K	C	D	F	G
0.1	$3.34\ 10^5$	$1.23\ 10^6$	$7.71\ 10^6$	$8.77\ 10^7$	$5.47\ 10^8$
0.05	$5.43\ 10^5$	$1.93\ 10^5$	$1.52\ 10^7$	$2.17\ 10^8$	$1.71\ 10^8$
0	1	5	60	1200	14400